

Micro-scale plastic deformation of polycrystalline Ti_3SiC_2 under room-temperature compression

Yanchun Zhou ^{*}, Zhimei Sun

Ceramic and Composite Department, Institute of Metal Research, Chinese Academy of Sciences, 72 Wenhua Road, Shenyang 110015, People's Republic of China

Received 9 March 2000; received in revised form 10 October 2000; accepted 24 October 2000

Abstract

The micro-scale plastic deformation of Ti_3SiC_2 ceramic under compression test was investigated. The results demonstrate that Ti_3SiC_2 is a damage tolerant material and samples are shear fractured upon failure. Micro-scale plastic deformation was observed in the local deformed region on the fractured surfaces. Owing to its complex crystal structure and insufficient number of slip systems, the deformation modes for polycrystalline Ti_3SiC_2 at room temperature are a combination of delamination and kink-band formation of elongated grains, dislocation slip and intergranular fracture, which result in micro-scale plasticity in polycrystalline Ti_3SiC_2 . © 2001 Elsevier Science Ltd. All rights reserved.

Keywords: Fracture; Mechanical properties; Plasticity; Ti_3SiC_2

1. Introduction

Titanium silicon carbide (Ti_3SiC_2) is a layered ternary compound, which is increasingly attractive to material scientists and physicists owing to its unique combination of properties. It has a high melting point, low density, good thermal¹ and electrical conductivity,² high strength and modulus,^{3–4} excellent thermal shock and high temperature-oxidation resistance.⁵ Table 1 lists the typical properties of Ti_3SiC_2 . Consequently, Ti_3SiC_2 and related ceramic materials are promising candidates for a range of high temperature applications. Therefore, it is important to understand the damage mechanism of Ti_3SiC_2 from the application point of view.

Damage mechanisms of Ti_3SiC_2 and/or Ti_3SiC_2 -based ceramics were investigated previously and micro-scale ductility and micro-damage have been the subject of a number of recent investigations,^{6–10} Gota and Hirai,⁶ Lis et al.⁷ and El-Raghy et al.⁸ measured the Vickers hardness of Ti_3SiC_2 and found it to decrease with increasing load and asymptotically to approach 4 GPa at the highest load. El-Raghy et al.⁸ investigated the damage around the indentation and observed no

indentation cracks at loads as high as 300 N. Low⁹ studied the nature, evolution and degree of deformation-microfracture damage around and beneath Vickers contacts in Ti_3SiC_2 . The work demonstrated that Ti_3SiC_2 exhibited a pronounced shear deformation during indentation. The deformation was accommodated by multiple intragrain slip and intergrain sliding which led to nucleation of subcritical voids or microcracks. The key to the damage tolerance lies in irreversible deformation and quasi-plasticity under conditions of intense compression-shear stress beneath the indenter. Zhou and Sun¹⁰ investigated the microstructure and mechanisms of damage tolerance for Ti_3SiC_2 . By monitoring the load-displacement curve and observing the crack propagation path of the single-edge-notched-beam specimen, they demonstrated that the damage tolerance mechanisms for Ti_3SiC_2 were basal plane slip, grain buckling, crack deflection, crack branching, pull-out and delamination of the laminated Ti_3SiC_2 grains. More recently, Barsoum et al.^{11–12} showed that large-grained, oriented polycrystalline sample of Ti_3SiC_2 deformed plastically at room temperature under compression. The sample they used was fabricated via a hot forging operation in a channel die, followed by a 24-h annealing at 1600°C. They proposed that the deformation mode for Ti_3SiC_2 was shear formation by dislocation arrays, cavitation, creation of dislocation walls and kink

^{*} Corresponding author. Tel.: +86-24-23843531, ext. 55180; fax: +86-24-23891320.

E-mail address: yczhou@imr.ac.cn (Y. Zhou).

Table 1
Properties of Ti_3SiC_2

Space group	$P6_3/mmc$
Lattice parameter	$a = 3.067 \text{ \AA}$; $c = 17.645 \text{ \AA}$
Density	4.52 g/cm^3
Young's modulus	326 GPa
Vickers hardness	4 GPa
Compressive strength	900 MPa (RT) 500 MPa (1150°C)
Tensile strength	200 MPa (RT)
Fracture toughness	$8.5 \text{ MPa m}^{1/2}$
Brittle-to-ductile transition temperature	1050°C
Electrical conductivity	$9.6 \times 10^6 \Omega^{-1} \text{ m}^{-1}$
Thermal conductivity	43 W/m K
Thermal expansion coefficient	$8.6 \times 10^{-6}/\text{K}$ (a -axes), $9.7 \times 10^{-6}/\text{K}$ (a -axes)
Oxidation resistance	$2 \times 10^{-8} \text{ kg}^2\text{m}^{-4} \text{ s}^{-1}$ (at 1000°C)

boundaries, buckling and delamination of Ti_3SiC_2 grains.

Previous work¹³ showed that the chemical bonding of Ti_3SiC_2 was metallic-covalent-ionic in nature and suggested that Ti_3SiC_2 ceramic might behave plastically under certain circumstance, for example, for oriented samples under compression load, as in the case of Barsoum and his co-workers.^{11–12} However, pure bulk Ti_3SiC_2 material is difficult to fabricate, not to say oriented or single crystal Ti_3SiC_2 . In fact, $\text{Ti}_3\text{SiC}_2/\text{TiC}$ ⁷ or $\text{Ti}_3\text{SiC}_2/\text{SiC}$ ¹⁴ composites demonstrated better mechanical properties than monolithic Ti_3SiC_2 . Recently, we fabricated polycrystalline Ti_3SiC_2 by a simple method of in-situ hot pressing/solid-liquid reaction.¹⁵ The polycrystalline material prepared by this method showed superior mechanical properties.¹⁵ In the present work, we investigate the micro-scale plastic deformation of polycrystalline Ti_3SiC_2 (containing 7 wt.% $\text{SiC} + \text{TiC}$) under compression test. The mechanisms for the micro-scale plastic deformation are discussed based on microstructure analysis.

2. Experimental

The material used in this work is polycrystalline Ti_3SiC_2 , TSC^{ZSS10}, which was fabricated by the in-situ hot pressing/solid-liquid reaction process.¹⁵ Briefly, the material was made according to the following procedure. Ti, Si and graphite powders were mixed and milled in a polypropylene jar for 10 h. After ball milling, the mixed powders were cold pressed into discs of 50 mm in a graphite die. The in-situ hot pressing/solid-liquid reaction was conducted under a flowing argon atmosphere in a furnace using graphite as heating element. The bulk material, TSC^{ZSS10}, was hot pressed at 1550°C under a pressure of 40 MPa for 60 min. The Ti_3SiC_2 content in TSC^{ZSS10} is 93 wt.% which was calculated using the Rietveld method.¹⁶

Samples for compressive testing are cylinders with 5.0 mm in diameter and 8.0 mm in height. The compressive test specimens were electrical-discharge machined from the bulk material without additional surface polish. The compressive tests were performed on a Gleeble-1500 universal-testing machine (Gleebe Inc., USA) at room temperature at a strain rate of $1 \times 10^{-4} \text{ s}^{-1}$. The fracture surfaces of the samples were examined in a s-360 scanning electron microscope equipped with energy dispersive spectroscopy (EDS) (Cambridge Instruments Ltd, UK). The deformed sample was also examined in transmission electron microscopy. The sample for TEM observation was made in the following procedure. Thin disc of 0.5 mm in thickness and 3 mm in diameter was cut by electrical-discharge method from the sample after room temperature compression testing, followed by mechanical thinning and polishing by a dimple grinder. Thin foils were made by ion beam milling at 5 kV using an incident angle of 15° . Microstructure observation was performed in a Philips EM-420 transmission electron microscope operated at 120 kV.

3. Results and discussion

The microstructure of the polycrystalline Ti_3SiC_2 prepared by the in-situ hot pressing/solid-liquid reaction process is shown in Fig. 1. A heterogeneous microstructure, which is analogous to that of platelet reinforced ceramic matrix composites, is seen in the figure. The material consists of large laminated grains and small equiaxial grains. The anisotropic and layered nature of the material is also revealed in Fig. 1. Previous work¹⁰ demonstrated that buckling, pull-out and delamination of the large laminated grains were the major contribution to the high toughness and damage tolerance of Ti_3SiC_2 .

Fig. 2 shows a typical room temperature compressive stress-strain curve of polycrystalline Ti_3SiC_2 . It is interesting to note that although no macro-plastic deformation can be observed in the experiment, the stress-strain curve deviated from linearity. The pseudo-strain for Ti_3SiC_2 upon failure under compressive load is about 5.7%. In fact, the polycrystalline Ti_3SiC_2 samples exhibited good resistance to damage during compressive tests. After reaching a stress of about 500 MPa, the sample underwent a number of cycles of loading-relaxation-reloading before failure. Another interesting phenomenon is that unlike most brittle ceramic materials which are broken into small pieces upon failure, polycrystalline Ti_3SiC_2 was not totally broken into small pieces but shear fractured. The above phenomena suggest that Ti_3SiC_2 is a damage tolerant material, undergoing micro-scale deformation during compressive testing. To understand the mechanisms of micro-scale deformation in polycrystalline Ti_3SiC_2 , the cracking

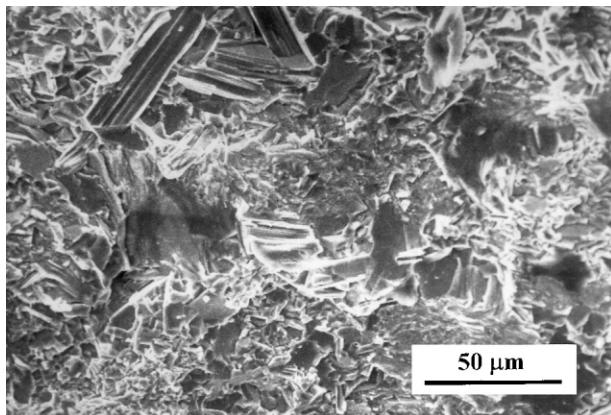


Fig. 1. Microstructure of polycrystalline Ti_3SiC_2 prepared by the in-situ hot pressing/solid-liquid reaction process.

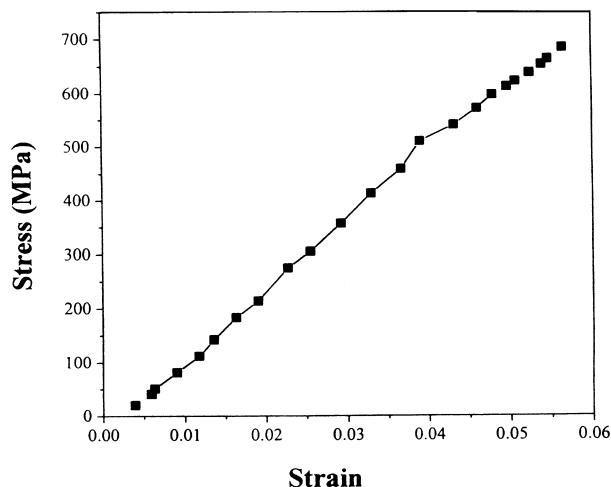


Fig. 2. Typical stress–strain curve of polycrystalline Ti_3SiC_2 under room temperature compression test, the strain rate is $1 \times 10^{-4} \text{ s}^{-1}$.

process and the fracture surface of the shear-fractured sample were examined.

Fig. 3(a) shows a scanning electron micrograph of a shear-fractured sample, wherein a crack which is oriented $\sim 45^\circ$ to the loading direction is seen. The figure also shows that although the sample is cracking, it is still not totally broken into small pieces. At high magnifications (right part of the figure), voids and cavities are seen and the crack is bridged by laminated Ti_3SiC_2 grains. Fig. 3(b) shows a scanning electron micrograph of the fracture surface of Ti_3SiC_2 after breaking the shear-fracture specimen into two parts. Two salient features can be identified from this figure. One is the shear deformation characteristic of laminated Ti_3SiC_2 grains, which can be seen from the delamination of the Ti_3SiC_2 grains. The other is that the laminated Ti_3SiC_2 grains are composed of a stack of nano-meter-size-thick hexagonal slices or micro-lamellae. The hexagonal slice or micro-lamella is the typical crystalline shape¹⁰ of layered compound Ti_3SiC_2 . Computer simulated crys-

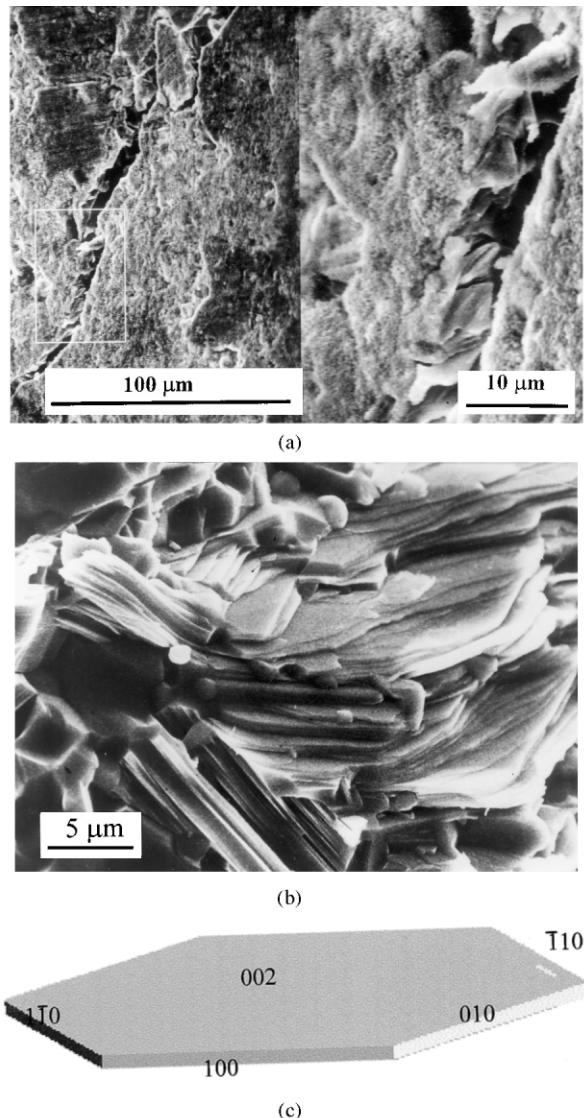


Fig. 3. (a) Scanning electron micrograph of a shear-fractured sample after loading, the left part is a low magnification of the shear-fractured sample surface and the right part is a high magnification micrograph of the rectangular area of the left part. (b) Scanning electron micrograph of the fracture surface of Ti_3SiC_2 after compressive loading. (c) Computer simulated crystallite shape of Ti_3SiC_2 , the top surfaces are parallel to $\{002\}$ and the side surfaces are parallel to $\{100\}$ planes of Ti_3SiC_2 .

tallite shape using the *Morphology* code in Cerius2 computational program for material research based on the Donnay–Harker¹⁷ theory reveals that the hexagonal surfaces are parallel to $\{002\}$ and the side surfaces are parallel to $\{100\}$ planes of Ti_3SiC_2 .¹⁰ Fig. 3(c) shows the computer simulated crystallite shape. The thin hexagonal slices or micro-lamellae constitute the laminated Ti_3SiC_2 grains. According to the Donnay–Harker theory,^{10,17} they are formed when the growth rate on $\{002\}$ surface is the slowest among that of $\{002\}$, $\{100\}$ and $\{101\}$ surfaces. These hexagonal slices of micro-lamellae are weakly bonded⁹ allowing easy shear slip. The weak

boundaries between the thin lamellae may also act to suppress macro-fracture by deflecting incipient surface cracks away from the directional tensile stress trajectories.⁹ The contribution of the laminated Ti_3SiC_2 grains to the micro-scale deformation will be discussed in the following section.

The SEM micrograph of micro-scale deformation region from the fracture surface of Ti_3SiC_2 is shown in Fig. 4(a) and (b). The later is a high magnification micrograph of the area marked A in Fig. 4(a). It is seen from the figure that kinking and delamination of individual grains [as marked A and B in Fig. 4(a)], together with intergranular fracture are the main deformation

mode of polycrystalline Ti_3SiC_2 under compression. The kinks in Fig. 4(b) demonstrate very sharp curvatures, usually with acute angle of 60° , and the sharp curvatures are always accompanied by strong delamination of the lamellae. Break-up of the laminated grain is also seen in Fig. 4(b) (as marked A). However, the delamination of Ti_3SiC_2 individual grains did not result in catastrophic failure because of the unusual capacity for Ti_3SiC_2 to confine the spatial extent of the damage. Some of the kinked individual grains fractured in the direction normal to the basal plane.

To understand the mechanism of the kinking and delaminating of individual grains in Ti_3SiC_2 , the formation of kink-bands is illustrated in Fig. 4(c). When the compressive stress is parallel to the basal plane, i.e. the $\{002\}$ planes of Ti_3SiC_2 , basal plane dislocations of the type $1/3[11\bar{2}0]$ will move at initial stage of loading to eliminate the local stress. The critical resolved shear stress in Ti_3SiC_2 at room temperature was estimated by Barsoum and El-Raghy to be 36 MPa.¹¹ The movement of basal plane dislocations has been observed in thin foil of Ti_3SiC_2 by transmission electron microscopy. Fig. 5(a) shows the slip trace of basal plane dislocations.

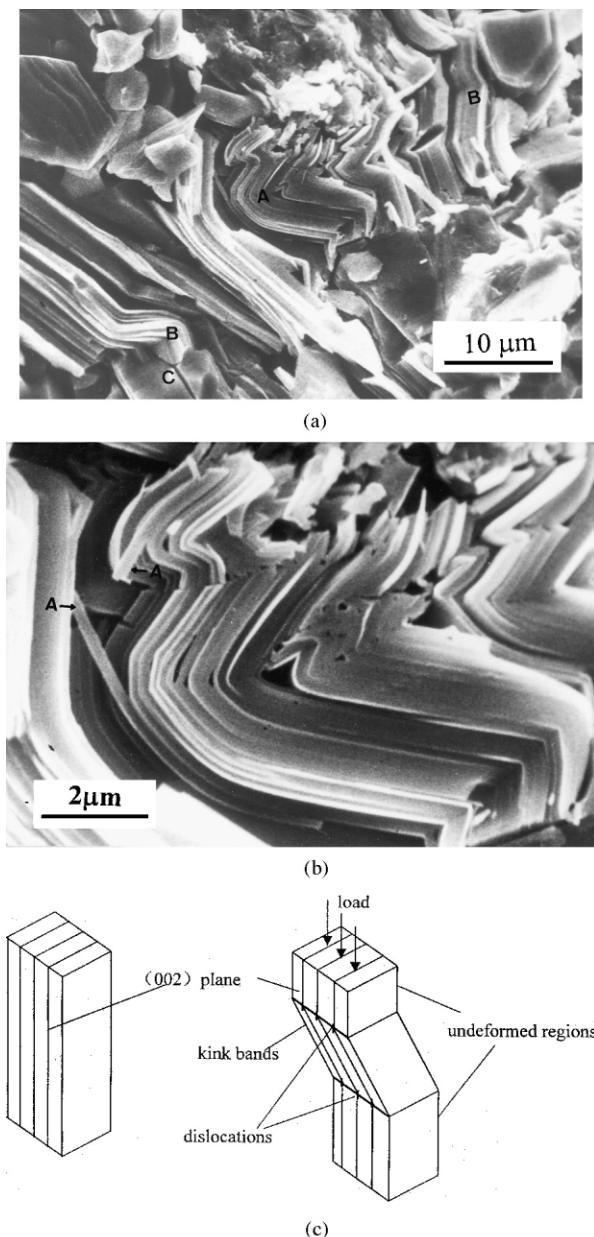


Fig. 4. (a) SEM micrograph of the local deformation region from fracture surface. (b) High magnification micrograph of the A part in Fig. 4(a). (c) Simulation of kink-band deformation model.

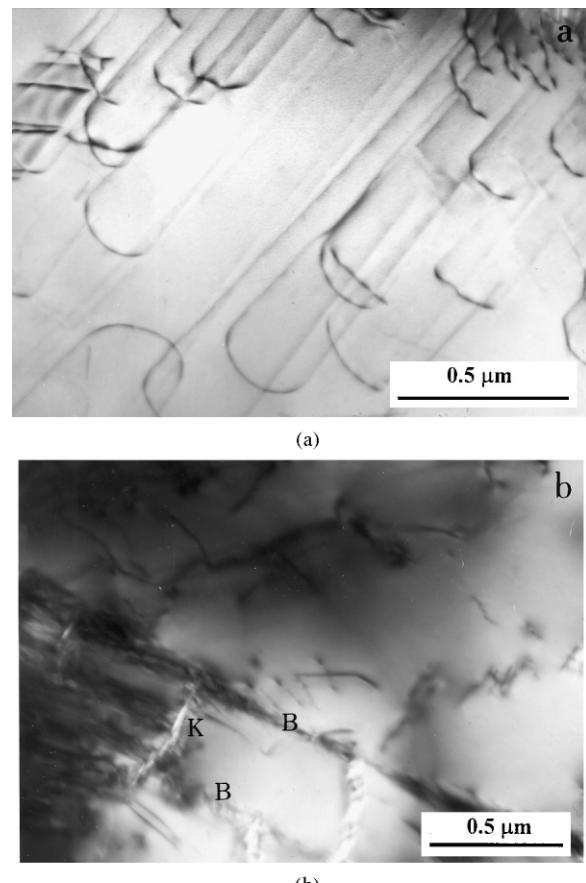


Fig. 5. (a) TEM micrograph showing slip trace of basal plane dislocations. (b) TEM micrograph showing that the kink boundary is normal to the basal plane of Ti_3SiC_2 .

These dislocations move throughout the entire grain of Ti_3SiC_2 and pile up at grain boundaries. Because no additional slip systems other than the basal plane dislocation are identified in hexagonal Ti_3SiC_2 , plastic deformation through basal plane slip can be observed only in single crystal or large grain size oriented Ti_3SiC_2 . When the compressive stress further increases, the parallel lamellae that are approximately equal in thickness, rotate to relax the stress because slip deformation is impossible due to small number of slip systems. If a cavity is formed locally, rotation of the lamellae will be easy and kink bands will be formed accompanying the delamination of the elongated grains. If there is no local cavity, rotation of the lamellae will be difficult and the local stress cannot be released, therefore only delamination of Ti_3SiC_2 grains but no kink bands will be formed. TEM observation suggests that the kink boundary, where a series of edge dislocations pile up, is nearly normal to the slip plane or the direction of compressive stress. Fig. 5(b) shows a TEM micrograph of deformed polycrystalline Ti_3SiC_2 . It is seen from the figure that the kink boundary (as marked K in the figure) is normal to the basal plane (as marked B in the figure). If the stress is normal to the lamellae, intergranular fracture occurs [as marked C in Fig. 4(a)]. Therefore, the deformation mode of polycrystalline Ti_3SiC_2 under compression are kink band formation and delamination of elongated grains, dislocation slip and intergranular fracture. The above analysis demonstrates that polycrystalline Ti_3SiC_2 exhibits micro-scale plasticity owing to the deformation modes of kinking and delamination and dislocation slip. The micro-scale plasticity in Ti_3SiC_2 results in local deformation in the compressive test samples.

4. Conclusion

The micro-scale plastic deformation in polycrystalline Ti_3SiC_2 ceramic was investigated by fractographic study of the compressive samples. The results demonstrate that Ti_3SiC_2 is a damage tolerant material. Micro-scale plastic deformation can be observed at the fracture surfaces. Owing to its complex crystal structure and small number of active slip systems, the deformation modes for polycrystalline Ti_3SiC_2 in room-temperature compression are a combination of delamination and kink-band formation of elongated grains, dislocation slip and intergranular fracture, which results in micro-scale plasticity in polycrystalline Ti_3SiC_2 .

Acknowledgements

This work was supported by the National Outstanding Young Scientist Foundation under Grant No. 59925208, the National Science Foundation of China (NSFC) under Grant No. 50072034, and '863' program.

References

1. Barsoum, M. and El-Raghy, T., Synthesis and characterization of a remarkable ceramic: Ti_3SiC_2 . *J. Am. Ceram. Soc.*, 1996, **79**, 1953–1956.
2. Sun, Z. and Zhou, Y., Ab initio calculation of titanium silicon carbide (Ti_3SiC_2). *Phys. Rev. B*, 1999, **60**, 1441–1443.
3. Zhou, Y. and Sun, Z., The compressive property and brittle-to-ductile transition of Ti_3SiC_2 ceramics. *Mater. Res. Innovat.*, 1999, **3**, 171–174.
4. Onodera, A., Hirano, H. and Yuasa, T., Static compression of Ti_3SiC_2 to 61 GPa. *Appl. Phys. Lett.*, 1999, **74**, 3782–3784.
5. Barsoum, M. and El-Raghy, T., Oxidation of Ti_3SiC_2 in air. *J. Electrochem. Soc.*, 1997, **14**, 2508–2516.
6. Goto, T. and Hirai, T., Chemical vapor deposited Ti_3SiC_2 . *Mater. Res. Bull.*, 1987, **22**, 2295–2302.
7. Lis, J., Miyamoto, R., Pampuch, R. and Tanihata, K., Ti_3SiC_2 -based materials prepared by HIP-SHS techniques. *Mater. Lett.*, 1995, **22**, 163–168.
8. El-Raghy, T., Zavaliangos, A., Barsoum, M. and Kalidindi, S., Damage mechanisms around hardness indentations in Ti_3SiC_2 . *J. Am. Ceram. Soc.*, 1997, **80**, 513–516.
9. Low, I., Vickers contact damage of micro-layered Ti_3SiC_2 . *J. Eur. Ceram. Soc.*, 1998, **18**, 709–713.
10. Zhou, Y. and Sun, Z., Microstructure and mechanism of damage tolerance for Ti_3SiC_2 bulk ceramic. *Mater. Res. Innovat.*, 1999, **2**, 360–363.
11. Barsoum, M. and El-Raghy, T., Room-temperature ductile carbides. *Metall. Mater. Trans. A*, 1999, **30**, 363–369.
12. Barsoum, M., Faber, L. and El-Raghy, T., Dislocations, kink bands, and room-temperature plasticity of Ti_3SiC_2 . *Metall. Mater. Trans. A*, 1999, **30**, 1227–1238.
13. Zhou, Y. and Sun, Z., Electronic structure and bonding properties of layered ternary carbide Ti_3SiC_2 . *J. Phys.: Condensed Matter*, 2000, **12**, 457–462.
14. Tong, X., Okano, T. and Iseki, T., Synthesis and high temperature mechanical properties of Ti_3SiC_2/SiC composites. *J. Mater. Sci.*, 1995, **30**, 3087–3090.
15. Zhou, Y., Sun, Z., Chen, S. and Zhang, Y., In-situ hot pressing/solid-liquid reaction synthesis of dense titanium silicon carbide ceramics. *Mater. Res. Innovat.*, 1998, **2**, 142–146.
16. Young, R., *The Rietveld Method*. Oxford University Press, Oxford, 1993.
17. Berkovitch-Yellin, Z., Toward an ab initio derivation of crystal morphology. *J. Am. Chem. Soc.*, 1985, **107**, 8239–8253.